η^2-Palladium and Platinum(II) Complexes of a λ^4-Phosphinine Anion: Syntheses, X-ray Crystal Structures, and DFT Calculations

Audrey Moores, Nicolas Mézailles, Louis Ricard, Yves Jean, and Pascal le Floch*

Laboratoire "Hétéroéléments et Coordination", UMR CNRS 7653, Ecole Polytechnique, 91128 Palaiseau Cedex, France

Received February 23, 2004

A 1-methyl-2,6-bis(trimethylsilyl)-3,5-diphenylphosphinine anion (**2**) reacts with $[MCl_2(PPh_3)_2]$ (M = Pd, Pt) to afford the corresponding η^2-palladium (**3**) and platinum (**4**) complexes in which coordination of the ligand to the $[MCl(PPh_3)]$ fragments occurs through the P−C bond. Complexes **3** and **4** were structurally characterized. Both complexes adopt the same stereochemistry, the Cl ligand lying *cis* to the carbon atom of the P−C bond. Variable-temperature NMR experiments demonstrate that in **3** and **4** the $[MCl(PPh_3)]$ fragment rapidly exchanges between the two P−C bonds in solution. DFT calculations on model complexes were performed to determine the structure of the transition state in the case of the palladium complex **3**. The value of the calculated $\Delta G^{\ddagger}$ is discussed regarding the experimental values obtained by NMR studies. IMOMM (DFT-MM3, QM/MM hybrid method) calculations were also carried out on the real systems to rationalize the stereochemistry of both complexes.

Introduction

It is now well established that phosphinines are suitable precursors of 1-R phosphahexadienyl anions through reaction of their electrophilic phosphorus atom with nucleophiles. This reactivity has been widely exploited in the synthesis of numerous λ^3-1,2- and λ^3-1,4-dihydrophosphinine and 1,1-λ^5-phosphinine derivatives (Scheme 1).[1]

However, only little attention has been paid to their reactivity toward metal fragments. Some authors have shown that these anions can coordinate transition metals through the carbocyclic part of the ring in an η^5-fashion, and two bis(1-R-2,4,6-trisubstituted phosphinine) iron complexes were structurally characterized.[2] Recently, with the aim to develop the use of these anionic ligands in coordination chemistry and catalysis, we reinvestigated their synthesis and their electronic structure through DFT calculations.[3] During this study, some η^5-lithium complexes of λ^4-phosphinine anions were synthesized and structurally characterized. Undoubtedly, the most significant feature of these λ^4-phosphinine anions is their ambidentate character that allows coordination through the anionic π-system (η^5) or through the lone pair (η^1) at phosphorus. However, some recent studies have shown that η^1-coordination at phosphorus is limited and exclusively occurs when ancillary ligands are present at the periphery of the ring to encapsulate the metal center. Thus a series of group 9[4] and group 10[5] complexes of SPS pincer ligands have recently been discovered and have found interesting applications in coordination chemistry and catalysis (Scheme 2).[6] To gain a better understanding of the factors that govern the coordination behavior of these anions (η^5-coordination versus η^1-coordination), we decided to investigate their reactivity toward metallic fragments that usually favor η^1-coordination. Therefore, we focused this study on Pd(II) and Pt(II) complexes. As will be seen, this investigation led us to discover a new bonding mode of these anions. Herein we report on these results.

Scheme 1

Scheme 2

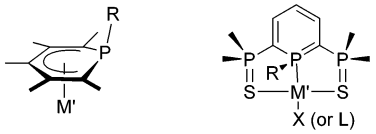

η^5-coordination η^1-coordination

(1) (a) Ashe, A. J. I.; Smith, T. W. *Tetrahedron Lett.* **1977**, 407−410. (b) Märkl, G.; Merz, A. *Tetrahedron Lett.* **1968**, 3611−3614. (c) Märkl, G.; Merz, A. *Tetrahedron Lett.* **1971**, 1215−1218. (d) Märkl, G.; Martin, C.; Weber, W. *Tetrahedron Lett.* **1981**, *22*, 1207−1210. (e) Dimroth, K. *Acc. Chem. Res.* **1982**, *15*, 58−64.

(2) (a) Markl, G.; Martin, C. *Angew. Chem., Int. Ed. Engl.* **1974**, *13*, 408−409. (b) Dave, T.; Berger, S.; Bilger, E.; Kaletsch, H.; Pebler, J.; Knecht, J.; Dimroth, K. *Organometallics* **1985**, *4*, 1565−1572. (c) Baum, G.; Massa, W. *Organometallics* **1985**, *4*, 1572−1574. (d) Nief, F.; Fischer, J. *Organometallics* **1986**, *5*, 877−883.

(3) Moores, A.; Ricard, L.; Le Floch, P.; Mézailles, N. *Organometallics* **2003**, *22*, 1960−1966.

(4) Doux, M.; Mézailles, N.; Ricard, L.; Le Floch, P. *Organometallics* **2003**, *22*, 4624−4626.

(5) (a) Doux, M.; Bouet, C.; Mézailles, N.; Ricard, L.; Le Floch, P. *Organometallics* **2002**, *21*, 2785−2788. (b) Doux, M.; Mézailles, N.; Ricard, L.; Le Floch, P. *Eur. J. Inorg. Chem.* **2003**, 3878−3894.

(6) Doux, M.; Mézailles, N.; Melaimi, M.; Ricard, L.; Le Floch, P. *Chem. Commun.* **2002**, 1566−1567.

10.1021/om049871y CCC: $27.50
Publication on Web 05/06/2004

Table 1. Crystal Data and Structural Refinement Details for Structures of Compounds 3 and 4

	3	4
cryst size [mm]	0.20 × 0.18 × 0.16	0.18 × 0.08 × 0.06
empirical formula	$C_{42}H_{47}ClP_2PdSi_2$	$C_{42}H_{47}ClP_2PtSi_2$
molecular mass	811.77	900.46
cryst syst	monoclinic	monoclinic
space group	$P2_1/c$	$P2_1/c$
a [Å]	12.7040(10)	12.6760(10)
b [Å]	18.8580(10)	18.9290(10)
c [Å]	17.2190(10)	17.2060(10)
α [deg]	90.00	90.00
β [deg]	106.4700(10)	106.4520(10)
γ [deg]	90.00	90.00
V [Å]^3	3955.9(4)	3959.4(4)
Z	4	4
calcd density [g·cm^{-3}]	1.363	1.511
abs. coeff [cm^{-1}]	0.707	3.781
$2\theta_{max}$ [deg]	30.03	30.03
F(000)	1680	1808
index ranges	−17 17; −23 26; −24 24	−17 17; −26 24; −24 24
no. of reflns collected/indep	18 799/11 507	20 690/11 539
no. of reflns used	8837	8329
R_{int}	0.0221	0.0340
abs corr	0.8716 min., 0.8953 max.	0.5493 min., 0.8049 max.
no. of params refined	440	440
refln/param	20	18
final R1[a]/wR2 [$I > 2\sigma(I)$][b]	0.0397/0.1148	0.0360/0.0734
goodness-of-fit on F^2	1.063	0.981
diff peak/hole [e·Å^{-3}]	1.386(0.093)/−1.254(0.093)	2.547(0.137)/−1.959(0.137)

[a] $R1 = \sum||F_o| - |F_c||/\sum|F_o|$. [b] $wR2 = (\sum w||F_o|^2 - |F_c|^2|^2/\sum w|F_o|^2)^{1/2}$.

Results and Discussion

All our experiments were conducted with the 2,6-bis-(trimethylsilyl)phosphinine **1**, a ligand that was already used in the synthesis of η^5-lithium complexes. Phosphinine **1** was chosen because of its availability and for the steric bulk provided by the two $SiMe_3$ groups that enhances kinetic stability.

Synthesis of anion **2** was carried out following a classical procedure that involves the reaction of a stoichiometric amount of MeLi at −78 °C in THF. The complete formation of **2** was checked by ^{31}P NMR. Addition of $[Pd(PPh_3)_2Cl_2]$ at low temperature followed by a very slow warming overnight to room temperature afforded complex **3**. Interestingly, the ^{31}P NMR spectrum of the crude mixture revealed the presence of free triphenylphosphine, indicating that an exchange of ligand had taken place. However, the formulation of **3** could not be unambiguously established by examination of its NMR data. Indeed, its ^{31}P NMR spectrum exhibits an AB system (12.35 ppm, 25.30 ppm, $^2J_{PP} = 31.7$ Hz), and its ^1H and ^{13}C NMR spectra (recorded at 25 °C) suggest that **3** adopts a symmetrical structure, the two trimethylsilyl groups being magnetically equivalent. Fortunately single crystals of **3** could be grown and an X-ray crystallographic study was undertaken. An ORTEP plot of one molecule of **3** is presented in Figure 1, and the most significant distances and angles are listed in Table 1. Contrary to the structure expected from the ^1H and ^{13}C NMR data, complex **3** is not symmetrical and features one $[PdCl(PPh_3)]$ fragment coordinated in an η^2-fashion onto one P−C bond of anion **2**. Note that this geometry is in good agreement with the ^{31}P NMR spectrum but disagrees with ^1H and ^{13}C NMR data. This quite unusual structure deserves further comment. First, the overall geometry around palladium is square planar, the Cl1 ligand and the C1 carbon being fixed in a *cis*-arrangement. The triphenylphosphine ligand points toward the less congested region of the molecule. It must be noted that no trace of the second isomer (P1 and P2 in a *trans* arrangement) could be detected during our experiments. Examination of bond distances and bond angles within the ring shows that the geometry of the

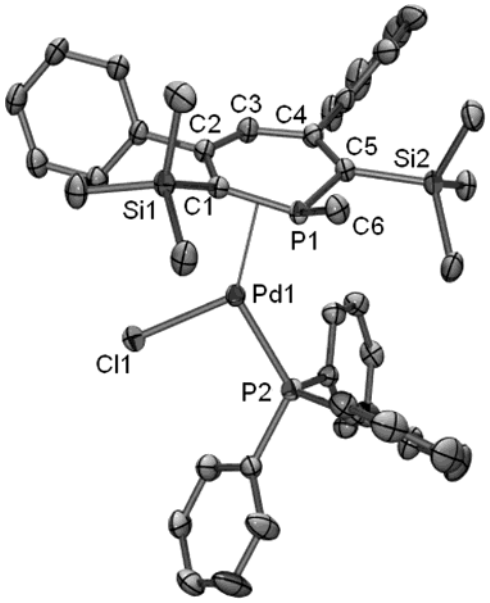

Figure 1. ORTEP view of one molecule of complex **3**. Ellipsoids are scaled to enclose 50% of the electron density. The numbering is arbitrary and different from that used in the assignment of NMR spectra. Relevant distances (Å) and bond angles (deg): Pd1−P1, 2.2014(6); Pd1−Cl1, 2.3930(6); Pd1−C1, 2.238(2); Pd1−P2, 2.3106(6); P1−C1, 1.775(2); P1−C5, 1.767(2); P1−C6, 1.824(2); C1−C2, 1.451(3); C2−C3, 1.377(3); C3−C4, 1.428(3); C4−C5, 1.386(3); P1−Pd1−C1, 47.12(6); P1−Pd1−P2, 111.09(2); C1−Pd1−Cl1, 104.10(6), P2−Pd1−Cl1, 97.75(2); C5−P1−C1, 112.3(1); C5−P1−C6, 109.5(1); C1−P1−C6, 116.2(1); C2−C1−P1, 113.4(2); C3−C2−C1, 124.5(2); C2−C3−C4, 127.9(2); C5−C4−C3, 124.5(2); C4−C5−P1, 115.4(2).

Scheme 3

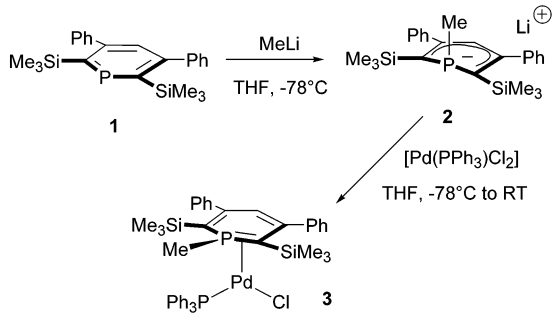

Scheme 4

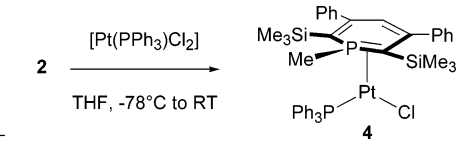

ring has been significantly modified upon coordination. Thus the two P−C bonds of the ring are shortened (P1−C1 = 1.775(2) Å, P1−C5 = 1.767(2) Å) by comparison with values recorded in the free anionic ligand [**2**][Li(THF)$_4$] (average 1.807 Å). The electronic delocalization that occurs in the carbocyclic part of the ring in the anionic ligand has been totally disrupted, and there is a clear alternation between short and long C−C bonds. Thus, whereas the C1−C2 (1.451(3) Å) and C3−C4 (1.428(3) Å) bond lengths are quite long, the C2−C3 (1.377(3) Å) and C4−C5 (1.386(3) Å) bond lengths are short. Interestingly, the pyramidality at phosphorus (sum of the C−P−C angles) is significantly reduced from 302.1° in [**2**][Li(THF)]$_4$ to 338.0° in complex **3**. There is a close structural analogy between the metallacycle in complex **3** (P−C bond distances and pyramidality at phosphorus) and those in observed phosphinomethanide complexes [(η^2-R$_2$P-CH$_2$)M] (M = Zr,[7] Pd,[8] Mo[9]] reported by Karsch, Bickelhaupt, and Cowley.

To complete this study, syntheses of analogous Ni and Pt complexes were also attempted. Various nickel(II) complexes ([Ni(PPh$_3$)$_2$Cl$_2$], [NiBr$_2$(DME)] + PPh$_3$ in a 1:1 ratio) were tested, but each experiment led to a mixture of compounds whose structures could not be established on the exclusive basis of ^{31}P NMR data. More satisfactory results were obtained by reacting anion **2** with the [Pt(PPh$_3$)$_2$Cl$_2$] complex (Scheme 4).

Suitable microcrystals of **4** could be obtained, and a X-ray crystallographic study was carried out. A view of one molecule of **4** is presented in Figure 2, and the most significant bond lengths and bond angles are listed in Table 1. As can be seen, the overall structure of **4** closely resembles that of complex **3**. The stereochemistry of the complex is the same, the C1 carbon atom and the Cl1 ligand being fixed in a *cis*-arrangement. Apart from the metal ligand bond distances, all metric parameters within the ring are close to those recorded in complex **3**.

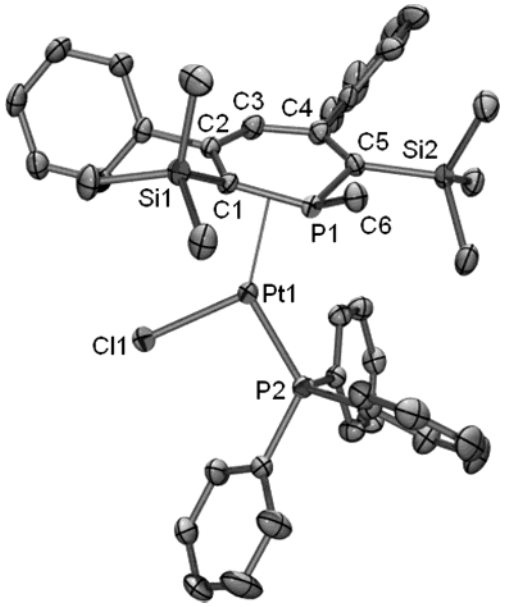

Figure 2. ORTEP view of one molecule of complex **4**. Ellipsoids are scaled to enclose 50% of the electron density. The numbering is arbitrary and different from that used in the assignment of NMR spectra. Relevant distances (Å) and bond angles (deg): Pt1−P1, 2.1915(8); Pt1−Cl1, 2.3803(8); Pt1−C1, 2.234(3); Pt1−P2, 2.2561(8); P1−C1, 1.794(3); P1−C5, 1.774(3); P1−C6, 1.821(3); C1−C2, 1.460(4); C2−C3, 1.382(4); C3−C4, 1.437(4); C4−C5, 1.373(4); P1−Pt1−C1, 47.8(1); P1−Pt1−P2, 111.99(3); C1−Pt1−Cl1, 102.6(1); P2−Pt1−Cl1, 97.64(3); C5−P1−C1, 112.5(2); C5−P1−C6, 108.7(2); C1−P1−C6, 116.3(1); C2−C1−P1, 112.7(2); C3−C2−C1, 124.7(3); C2−C3−C4, 128.3(3); C5−C4−C3, 124.3(3); C4−C5−P1, 115.9(2).

Interestingly, the lack of symmetry is not reflected in the ^{1}H and ^{13}C NMR spectra, which exhibit a broad single signal for the trimethylsilyl group as well as for the carbon atoms and substituents (^{13}C). Suspecting that **3** and **4** exist in solution as two enantiomeric complexes involved in a rapid equilibrium, a variable-temperature ^{1}H NMR study was undertaken. This experiment was carried out on complexes **3** and **4** (in CD_2Cl_2 for **3**, THF-d_8 for **4**). As expected, cooling solutions of **3** or **4** revealed that a dynamic process takes place. At −20 °C, for complex **3**, the signal of the trimethylsilyl groups significantly broadens and coalescence was observed at −48 °C. Below this temperature, two distincts signals could be observed. At −65 °C, signals (−0.555 and −0.048 ppm) are fine enough to calculate a free energy of 43.7 kJ·mol^{-1} for the exchange. For the platinum complex **4**, the coalescence temperature is −8 °C and the difference of frequency between the two signals was measured at −40 °C (−0.421 and −0.006 ppm), indicating a $\Delta G^{\ddagger}$ value of 55.5 kJ·mol^{-1} (Scheme 5, Figure 3).[10]

To shed some light on this mechanism as well as on the stereochemistry of **3** and **4**, DFT-B3LYP calculations (see Theoretical Methods) were first carried out on four model structures, **Ia**,**b** and **IIa**,**b**, **a** and **b** referring to two different stereochemical arrangements around the metal atom, Pd (**I**) or Pt (**II**) (Scheme 6). To save computation time, the triphenylphosphine ligand was replaced by a PH$_3$ ligand, the phenyl groups at the

(7) (a) Karsch, H. H.; Grauvogl, G.; Kawecki, M.; Bissinger, P.; Kumberger, O.; Schier, A.; Muller, G. *Organometallics* **1994**, *13*, 610−618. (b) Karsch, H. H.; Grauvogl, G.; Deubelly, B.; Muller, G. *Organometallics* **1992**, *11*, 4238−4245.

(8) van der Sluis, M.; Beverwijk, V.; Termaten, A.; Bickelhaupt, F.; Kooijman, H.; Spek, A. L. *Organometallics* **1999**, *18*, 1402−1407.

(9) Carrano, C. J.; Cowley, A. H.; Nunn, C. M.; Pakulski, M.; Quashie, S. *J. Chem. Soc., Chem. Commun.* **1988**, 170−171.

(10) For $\Delta G^{\ddagger}$ formula see Supporting Information and Günther, H. *NMR Spectroscopy*; Wiley: New York, 1980.

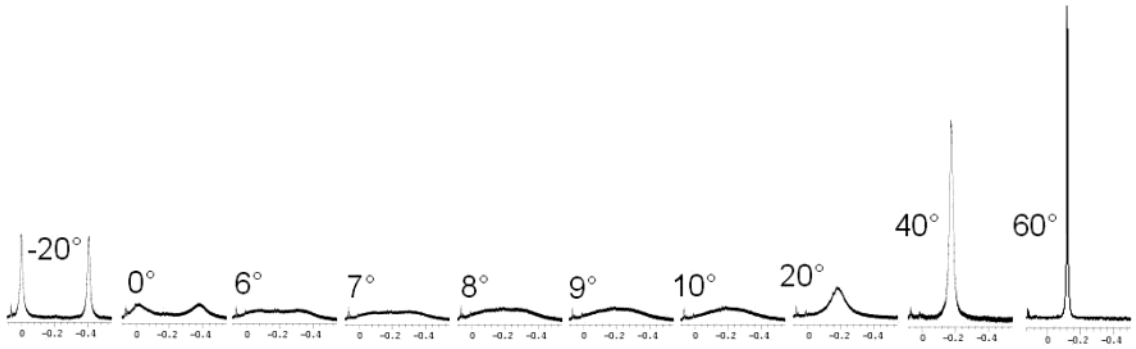

Figure 3. Variable-temperature NMR spectra (in ppm) of compound **4** in d_8-THF.

Scheme 5

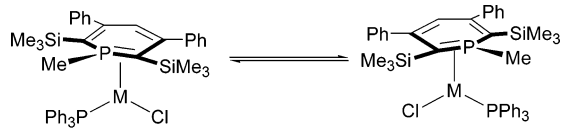

3: M = Pd; $\Delta G^{\#}$ = 43.7 kJ.mol^{-1}
4: M = Pt; $\Delta G^{\#}$ = 55.5 kJ.mol^{-1}

Scheme 6

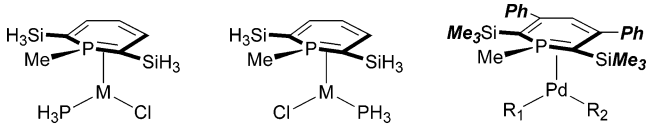

Ia: M = Pd
IIa: M = Pt

Ib: M = Pd
IIb: M = Pt

III: R_1=P***Ph***$_3$, R_2=Cl
IV: R_1=Cl, R_2=P***Ph***$_3$

Table 2. Distances and Angles within the DFT Optimized Structures Ia, Ib, IIa, IIb, and IaTS

	Ia (M = Pd)	**Ib** (M = Pd)	**IIa** (M = Pt)	**IIb** (M = Pt)	**IaTS** (M = Pd)
M−P(1)	2.264	2.256	2.248	2.268	2.253
M−Cl(1)	2.435	2.408	2.443	2.423	2.401
M−C(1)	2.240	2.259	2.245	2.218	
M−P(2)	2.347	2.421	2.294	2.345	2.297
P(1)−C(1)	1.787	1.790	1.798	1.806	1.765
P(1)−C(5)	1.775	1.772	1.781	1.784	1.765
P(1)−C(6)	1.840	1.836	1.838	1.837	1.843
C(1)−C(2)	1.440	1.442	1.450	1.456	1.401
C(2)−C(3)	1.378	1.376	1.372	1.368	1.400
C(3)−C(4)	1.425	1.426	1.431	1.435	1.400
C(4)−C(5)	1.382	1.381	1.379	1.374	1.401
C(1)−P(1)−C(5)	109.1	109.2	109.2	109.2	107.2
C(1)−P(1)−C(6)	116.4	118.1	117.4	118.2	112.6
C(5)−P(1)−C(6)	111.0	111.6	110.4	110.5	112.6
P(1)−M−C(1)	46.73	46.71	47.17	47.47	

β-position were replaced by H atoms, and the trimethylsilyl groups were replaced by SiH_3 groups.

The theoretical parameters for **Ia** and **IIa** were found to be in good agreement with the experimental values in **3** and **4** (see Table 2). More precisely, bond lengths and bond angles within the ring are nicely reproduced, while the metal−ligand distances are overestimated at most by 0.06 Å. The structure of **IaTS**, the transition state for the interconversion between the two enantiomeric Pd complexes **Ia** and **Ia′** (image of **Ia** with respect to the symmetry plane of the phosphinine ring, Scheme 7), is presented in Figure 4, and bond lengths and bond angles are given in Table 2. In this structure, the palladium fragment is bound in an η^1-fashion to the phosphorus atom of the phosphinine, so that this ligand can be described as a λ^5-phosphinine with the metal

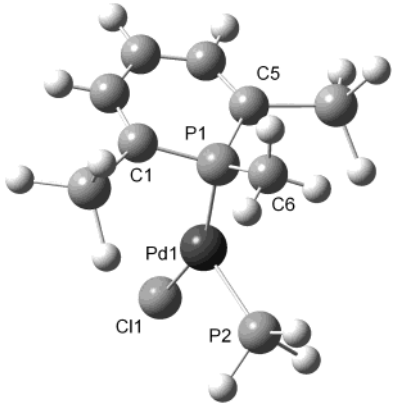

Figure 4. Transition state **IaTS** of the interconversion between the two enantiomeric Pd complexes **Ia** and **Ia′**.

Scheme 7

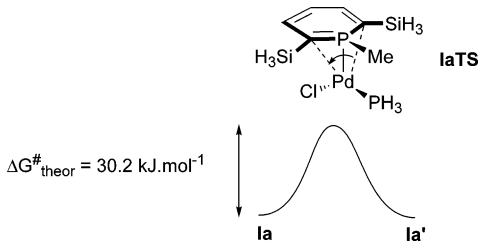

fragment as an axial substituent. The metal, chloride, and the phosphorus (PH_3) atoms are in the symmetry plane of the phosphinine ring, the chloride ligand being located below the ring plane. The environment around the metal is T-shaped with a large P1−Pd1−Cl1 angle, which is consistent with a d^8-ML_3 complex. C−C bond lengths within the phosphinine ring are now essentially identical (between 1.400 and 1.401 Å), whereas P−C distances have decreased from 1.787 and 1.775 Å in **Ia** structure to 1.765 Å; this accounts for a delocalization of the negative charge held by the ligand in **IaTS**. This interconversion process thus involves a change in the coordination mode of the ligand (from η^2 to η^1 and back to η^2) accompanied by a rotation of the whole [$PdPH_3$-Cl] fragment around the P1−Pd1 bond. The agreement between the $\Delta G^{\ddagger}$ theoretical value (30.2 kJ·mol^{-1}) and the experimental one (43.7 kJ·mol^{-1}) seems reasonable taking into account that these calculations were performed on a simplified model.

A series of calculations were also performed to rationalize the absence of the isomer of **3** adopting a *trans* arrangement between the two phosphorus centers. For the unsubstituted model complexes **Ia** (*cis*) and **Ib** (*trans*), the calculated DFT-B3LYP energy difference of

6.3 kJ·mol^{-1} (ΔG = 2.6 kJ·mol^{-1}) in favor of **Ia** is actually too small to rationalize the absence of the *trans* isomer. However, complexes **Ia** and **Ib** are only models, and as trimethylsilyl and triphenylphosphine substituents are replaced by SiH_3 and PH_3, respectively, steric congestion cannot be reproduced reasonably. The *cis* (**III**) and *trans* (**IV**) isomers with the experimental substituents were thus studied by means of QM/MM calculations using the IMOMM program.[11] In these calculations, the QM part was made of the model systems (namely, complex **Ia** for **III** and **Ib** for **IV**), the remaining part of the molecule (the phenyl groups and the methyl groups of trimethylsilyl substituents) being described at the MM3 level (substituents drawn in bold in Scheme 6). Surprisingly, the energy difference falls down to 3.8 kJ·mol^{-1}, a result that makes unlikely the hypothesis about steric interactions at work in the *trans* isomer **IV**. Finally, single-point energy calculations were performed at the DFT-B3LYP level using the IMOMM geometries. The *cis* isomer was now found to be more stable by 14.6 kJ·mol^{-1}, a value large enough to account for the experimental absence of the *trans* isomer (less than 1% according to the theoretical value). These sets of results show that a clear preference for the *cis* isomer is reproduced only if the actual substituents are introduced and calculated at the QM level. The failure of QM/MM calculations to give a significant energy difference between the two isomers might be due to the pure MM description of the phenyl groups. On the other hand, these calculations do not take into account solvation effect which might change the relative energies of the two isomers. However recent DFT studies on [M(PMe_3)$_2$$X_2$] complexes (M = Pd, Pt; X = Cl, Br, I) showed that polar solvents always tend to favor the *cis* isomer versus the *trans* one, due to the smaller dipole moment of the latter.[12]

Conclusion

We synthesized the first Pd and Pt(II) complexes where a 1-methyl-phosphacyclohexadienyl anion is coordinated in an η^2-fashion to the metal. A rapid exchange of the metal fragment between the two P−C bonds of the ring was evidenced by variable-temperature NMR experiments, and the structure of the transition state was determined by DFT calculations. We believe that this new coordination mode of phosphacyclohexadienyl anions can be extended to other metal fragments. Studies aimed at determining factors that favor η^2-coordination versus η^5-coordination through the carbocyclic π-system of the ring are currently underway in our laboratories.

Experimental Section

All reactions were routinely performed under an inert atmosphere of argon or nitrogen by using Schlenk and glovebox techniques and dry deoxygenated solvents. Dry THF, ether, and hexanes were obtained by distillation from Na/benzophenone. Dry dichloromethane was distilled over P_2O_5. Nuclear magnetic resonance spectra were recorded on a Bruker AC-200 SY spectrometer operating at 300.0 MHz for ^{1}H, 75.5 MHz for ^{13}C, and 121.5 MHz for ^{31}P. Solvent peaks are used as internal reference relative to Me_4Si for ^{1}H and ^{13}C chemical shifts (ppm); ^{31}P chemical shifts are relative to a 85% H_3PO_4 external reference. Coupling constants are given in hertz. The following abbreviations are used: s, singlet; d, doublet; t, triplet; m, multiplet. Methyllithium in ether solution was purchased from Fluka. Phosphinine **1** was prepared following procedures described in the literature.[13] Elemental analyses were performed by the "Service d'analyses du CNRS" at Gif sur Yvette.

Synthesis of 3. A solution of phosphinine **1** (50 mg, 0.13 mmol) in THF (2 mL) was prepared. A solution of MeLi in ether (80 μL, 0.13 mmol, 1.6 M) was added at −78 °C. The solution turned from colorless to red. The solution was warmed to room temperature, and completion of the reaction was checked by ^{31}P NMR. [$PdCl_2(PPh_3)_2$] (89 mg, 0.13 mmol) was then added at −78 °C. The solution was stirred at this temperature for 6 h. The solution was further left, allowing the cold bath to warm to room temperature over a period of 14 h. The solution was then orange. Lithium salts were removed by CH_2Cl_2 extraction (3 × 5 mL). After solvent removal, the orange solid was washed with ether (3 × 5 mL). The product was recovered as a yellow powder (87 mg, 84% yield), decomposition > 220 °C. Anal. Calcd for $C_{42}H_{47}ClP_2PdSi_2$: C, 62.14; H, 5.84. Found: C, 62.30; H, 5.91. ^{1}H NMR ($CDCl_3$): −1.15 (s, 18 H, Si−(CH_3)$_3$), 1.82 (d, $^2J_{HP}$ = 12.3 Hz, 3 H, P−CH_3), 6.34 (d, $^4J_{HP}$ = 5.9 Hz, 1 H, H_{para}), 7.33−7.74 (m, 25 H, C*H* of phenyls). ^{13}C{^{1}H} NMR ($CDCl_3$): 3.23 (s, Si−(CH_3)$_3$), 11.5 (dd, $^1J_{PC}$ = 40.6 Hz, $^3J_{PC}$ = 11.1 Hz, P-CH_3), 124.33 (dd, $^3J_{PC}$ = 29.2 Hz, $^4J_{PC}$ = 9.7 Hz, C_{para}H), 127.59, 130.61 (2 s, *C*H of phenyls), 128.16 (s, *C*H of PPh_3), 128.30, 134.64 (2 d, J_{PC} = 10.1, 13.6 Hz, *C*H of PPh_3), 129.68 (t, $\sum J_{PC}$ = 24.7 Hz, C_{ortho}−TMS), 130.23 (d, J_{PC} = 1.7 Hz, *C*H of phenyls), 133.47 (d, $^1J_{PC}$ = 36.1 Hz, C_{ipso} of PPh_3), 145.27 (d, $^2J_{PC}$ = 14.9 Hz, C_{meta}−Ph), 158.17 (dd, $^3J_{PC}$ = 8.3 Hz, $^4J_{PC}$ = 3.8 Hz, C_{ipso} of phosphinine phenyls). ^{31}P{^{1}H} NMR ($CDCl_3$): 12.35 (d, $^2J_{PP}$ = 31.7 Hz, P of phosphinine), 25.30 (d, $^2J_{PP}$ = 31.7 Hz, P of PPh_3).

Synthesis of 4. To a solution of phosphinine **1** (50 mg, 0.13 mmol) in THF (2 mL) was added a solution of MeLi in ether (80 μL, 0.13 mmol, 1.6 M) at −78 °C. The solution turned from colorless to red. The solution was warmed to room temperature, and completion of the reaction was checked by ^{31}P NMR. [$PtCl_2(PPh_3)_2$] (100 mg, 0.13 mmol) was then added at −78 °C. The solution was stirred at this temperature for 6 h. The solution was further left, allowing the cold bath to warm to room temperature over a period of 14 h. The solution was then brown. Lithium salts were removed by CH_2Cl_2 extraction (3 × 5 mL). After solvent removal, the brown solid was washed with hexanes (3 × 5 mL) and ether (3 × 5 mL). The product was recovered as a pale green powder (93 mg, 81% yield), decomposition > 220 °C. Anal. Calcd for $C_{42}H_{47}ClP_2PtSi_2$: C, 56.02; H, 5.26. Found: C, 55.76; H, 5.53. ^{1}H NMR (THF-d_8, 60 °C): −1.12 (s, 18 H, Si−(CH_3)$_3$), 1.93 (dd, $^2J_{HP}$ = 12.3 Hz, $^4J_{HP}$ = 0.95 Hz, 3 H, P−CH_3), 6.03 (d, $^4J_{HP}$ = 4.8 Hz, 1 H, H_{para}), 7.19−7.81 (m, 25 H, C*H* of phenyls). ^{13}C{^{1}H} NMR (THF-d_8, 20 °C): 4.84 (bs, Si−(CH_3)$_3$), 13.29 (dd, $^1J_{PC}$ = 42.0 Hz, $^3J_{PC}$ = 5.6 Hz, P−CH_3), 124.99 (dd, $^3J_{P-C}$ = 26.5 Hz, $^4J_{P-C}$ = 7.4 Hz, C_{para}H), 127.92−137.45 (m, *C*H of phenyls and C_{ortho}−TMS), 142.00 (bs, C_{meta}−Ph), 147.97 (bs, C_{ipso} of phenyls). ^{31}P{^{1}H} NMR (THF-d_8, 20 °C): −18.07 (d with satellites, $^1J_{PPt}$ = 2792.98 Hz, $^2J_{PP}$ = 24.1 Hz, P of phosphinine), 26.73 (td, $^1J_{PPt}$ = 4752.21 Hz, $^2J_{PP}$ = 24.1 Hz, P of PPh_3).

Theoretical Methods. Geometry optimizations and single-point energy-only calculations were carried out using the density functional theory (DFT)[14,15] by means of a pure

(11) Maseras, F.; Morokuma, K. *J. Comput. Chem.* **1995**, *16*, 1170−1179.

(12) Harvey, J. N.; Heslop, K. M.; Orpen, A. G.; Pringle, P. G. *Chem. Commun.* **2003**, 278−279.

(13) (a) Avarvari, N.; LeFloch, P.; Mathey, F. *J. Am. Chem. Soc.* **1996**, *118*, 11978−11979. (b) Avarvari, N.; LeFloch, P.; Ricard, L.; Mathey, F. *Organometallics* **1997**, *16*, 4089−4098.

(14) Parr, R. G.; Yang, W. *Density Functional Theory of Atoms and Molecules*; Oxford University Press: Oxford, U.K., 1989.

gradient-corrected exchange functional and the Lee−Yang−Parr nonlocal correlation functional BLYP[16] as implemented in the Gaussian 98 program.[17] A quasi-relativistic effective core potential operator was used to represent the electron core of the palladium and the platinium atom. The basis set for the metal was that associated with the pseudopotential with a standard double-ζ LANL2DZ contraction.[18] 6-31G* basis set was used for C, Si, P, and Cl atoms and the 6-31G basis set for H atoms.[19] The stationary points (minima, transition states) located at the DFT-B3LYP level were characterized by frequency calculations. The IMOMM set of programs (QM/MM calculation) was also used to optimize full size complexes, the QM part being described at the DFT-B3LYP level with the basis set detailed above and the MM part by the MM3 force field.[11]

X-ray Structural Determination. Pale yellow plates of complex **3** crystallized by diffusing hexanes into a dichloromethane solution of the complex **3**. Yellow needles of isomorphous complex **4** were obtained by slow evaporation of a THF solution of complex **4**. Data were collected on a Nonius Kappa CCD diffractometer using a Mo Kα (λ = 0.71070 Å) X-ray source and a graphite monochromator at 150 K. Experimental details are described in Tables 1 and 2. The crystal structures were solved using SIR 97[20] and SHELXL-97.[21] ORTEP drawings were made using ORTEP III for Windows.[22] These data can be obtained free of charge at www.ccdc.cam.ac.uk/conts/retrieving.html [or from the Cambridge Crystallographic Data Centre, 12, Union Road, Cambridge CB2 1EZ, UK; fax: (internat.) +44-1223/336-033; e-mail: deposit@ccdc.cam.ac.uk].

Acknowledgment. The authors thank Agusti Lledos for fruitful discussions. Feliu Maseras is also acknowledged for providing the IMOMM set of programs. The CNRS and the Ecole Polytechnique are thanked for supporting this work. The use of computational facilities of the French Institute IDRIS is gratefully acknowledged. This research was partially supported by the Improving Human Potential Programme, Access to Research Infrastructures under contract HPRI-1999-00071, "Access to CESCA and CEPBA Large-Scale Facilities" established between the European Community and CESCA-CEPBA. The Spanish "Dirección General de Investigación" (Project BQU2002-04110-CO2-02) is also acknowledged.

Supporting Information Available: Tables of crystal data, atomic coordinates and equivalent isotropic displacement parameters, bond lengths and bond angles, anisotropic displacement parameters, and hydrogen coordinates, ORTEP view of one molecule of compounds **3** and **4**; details on variable-temperature NMR; a listing of coordinates for calculated structures **Ia**,**b**, **IIa**,**b**, **IaTS**, and IMOMM optimized **III** and **IV**; optimized energies for structures **Ia**,**b**, **IIa**,**b**, **IaTS**, **III**, and **IV**. This material is available free of charge via the Internet at http://pubs.acs.org.

OM049871Y

(15) Ziegler, T. *Chem. Rev.* **1991**, *91*, 651−667.
(16) (a) Becke, A. D. *Phys. Rev. A* **1988**, *38*, 3098−3108. (b) Perdew, J. P. *Phys. Rev. B* **1986**, *33*, 8822−8832.
(17) Frisch, M. J.; Trucks, G. W.; Schlegel, H. B.; Scuseria, G. E.; Robb, M. A.; Cheeseman, J. R.; Zakrzewski, V. G.; Montgomery, J. J. A.; Stratmann, R. E.; Burant, J. C.; Dapprich, S.; Millam, J. M.; Daniels, A. D.; Kudin, K. N.; Strain, M. C.; Farkas, O.; Tomasi, J.; Barone, V.; Cossi, M.; Cammi, R.; Mennucci, B.; Pomelli, C.; Adamo, C.; Clifford, S.; Ochterski, J.; Petersson, G. A.; Ayala, P. Y.; Cui, Q.; Morokuma, K.; Malick, D. K.; Rabuck, A. D.; Raghavachari, K.; Foresman, J. B.; Cioslowski, J.; Ortiz, J. V.; Baboul, A. G.; Stefanov, B. B.; Liu, G.; Liashenko, A.; Piskorz, P.; Komaromi, I.; Gomperts, R.; Martin, R. L.; Fox, D. J.; Keith, T.; Al-Laham, M. A.; Peng, C. Y.; Nanayakkara, A.; Challacombe, M.; Gill, P. M. W.; Johnson, B.; Chen, W.; Wong, M. W.; Andres, J. L.; Gonzalez, C.; Head-Gordon, M.; Replogle, E. S.; Pople, J. A. In *Gaussian 98*, revision A-11; Gaussian, Inc.: Pittsburgh, PA, 1998.
(18) Hay, P. J.; Wadt, W. R. *J. Chem. Phys.* **1985**, *82*, 299−310.
(19) (a) Hehre, W. J.; Ditchfield, R.; Pople, J. A. *J. Chem. Phys.* **1972**, *56*, 2257. (b) Harihara, P.; Pople, J. A. *Theor. Chim. Acta* **1973**, *28*, 213−222. (c) Francl, M. M.; Pietro, W. J.; Hehre, W. J.; Binkley, J. S.; Gordon, M. S.; DeFrees, D. J.; Pople, J. A. *J. Chem. Phys.* **1982**, *77*, 3654−3665.
(20) Altomare, A.; Burla, M. C.; Camalli, M.; Cascarano, G.; Giacovazzo, C.; Guagliardi, A.; Moliterni, A. G. G.; Polidori, G.; Spagna, R. *SIR97, an integrated package of computer programs for the solution and refinement of crystal structures using single-crystal data.*
(21) Sheldrick, G. M. *SHELXL-97*; Universität Göttingen: Göttingen, Germany, 1997.
(22) Farrugia, L. J. *ORTEP-3*; Department of Chemistry: University of Glasgow.